Biophysical Chemistry, 30 (1988) 199–224
Elsevier

BPC 01257

Minireview

Anisotropy decay of fluorescence as an experimental approach to protein dynamics

Enrico Bucci [a] and Robert F. Steiner [b]

[a] *Department of Biochemistry, University of Maryland at Baltimore, 660 W. Redwood St, Baltimore, MD 21201 and* [b] *Department of Chemistry, University of Maryland, Baltimore County, Wilkens Ave., Catonsville, MD 21228, U.S.A.*

Received 17 November 1987
Revised manuscript received 17 February 1988
Accepted 17 February 1988

Anisotropy decay; Fluorescence anisotropy; Rotational correlation time; Protein flexibility; Allosteric protein

This minireview makes an initial assessment of the progress made using anisotropy decay measurements for investigating the conformational changes and molecular dynamics in soluble systems. A critical analysis of available data is presented. The anisotropy decays of the tryptophan fluorescence of staphylococcal nuclease, adrenocorticotropin, melittin and of labeled transfer RNA were studied for investigating the functional conformational changes of these systems. The emissions of variously labeled immunoglobulins have been used to elucidate the conformations of these proteins before and after the binding of specific antibodies. Labeled myosin and its fragments have given information on the functional motions of the protein domains. The anisotropy decays of labeled and natural hemoglobin systems have been utilized for exploring the allosteric behavior of these molecules. The data suggest a wide applicability of this technique to the study of protein dynamics and conformational changes of macromolecules.

1. Introduction

The formulation in 1965 of the Monod-Wyman-Changeaux thermodynamic model for allosteric systems made it clear that the biological function of proteins is regulated and modulated, to the 'instant' necessities of biosystems, by programmed conformational changes within the protein molecules [1].

In a simple-minded way allosteric systems may be conceived as molecular machines composed of various protein domains whose relative positions define the conformational attitudes of the system as programmed by the protein structure. The program is triggered by the interaction of the protein with allosteric effectors. The binding sites are its keyboard.

Many other proteins, for example, immunoglobulins and the muscle proteins, exert their biological activity through extensive modifications of their morphology.

It may be expected that these proteins are endowed with internal flexibilities defining regions of more compact structure capable of autonomous librational motions within the protein molecule. It is also possible that conformational changes are a diffuse property of the whole molecule, which should in this case behave like flexible polymers.

Elucidation of the mechanisms by which functional conformational changes take place in pro-

Correspondence address: E. Bucci, Department of Biochemistry, University of Maryland at Baltimore, 660 W. Redwood St. Baltimore, MD 21201, U.S.A.

Abbreviations: IAEDANS, *N*-iodoacetylaminoethyl-5-naphthylamine-1-sulfonate; ANS, 1-anilino-8-naphthalenesulfonate; PLP, pyridoxal 5′-phosphate; DNS, dansyl chloride. ϵ-ADP, etheno-adenosine diphosphate; IHP, inositol hexaphosphate.

teins has stimulated a great deal of research in the field of protein dynamics, in the attempt to explore the characteristics of the thermal motions which are at the basis of these conformational changes.

Recently the development of sophisticated spectroscopic equipment is providing investigators with the necessary tools for exploring the internal motions of proteins in the nano- and picosecond ranges, in real solutions and real time, rather then by computer simulations in ideal solutions and time projections. The time-dependent anisotropy of fluorescence emission provides this information by exploring the characteristics of rotational diffusion of emitting probes in solution. If the probe is part of a macromolecule the decay of its anisotropy will reveal whether the macromolecule behaves like a rigid rotor, a flexible polymer, or as a structured conglomerate of domains capable of independent librational behavior.

There is a wealth of new information emerging in the literature with regard to the time-dependent characteristics of emission of fluorescence and the time seems to be ripe for making an initial assessment of the progress made thus far and of that promised using this technique.

The intention in this minireview is to provide an overview of the information which can be obtained by analyzing the time-dependent anisotropy of the emission of intrinsic and extrinsic probes in proteins and polypeptides. Special emphasis is given to allosteric systems.

2. Theory of anisotropy decay

2.1. The meaning of anisotropy

Two basic kinds of information may be derived from fluorescence anisotropy decay measurements [2–5]. To the extent that the macromolecule and the attached label rotate as a unit, anisotropy decay may provide information as to the size and shape factor of the macromolecule. It is also a convenient means of studying any internal rotational motions present in the macromolecule and of examining the nature of the molecular flexibility.

The radiation emitted by a fluorophore may be polarized to varying extents, depending upon the conditions. The polarization is conventionally characterized with reference to a system of laboratory coordinates defined by the directions of observation and of the exciting beam. It is customary to observe the fluorescence at an angle of 90° to the exciting beam. If the center of the irradiated volume is chosen as the origin, O, and the x- and y-axes are taken along the direction of observation and of the exciting beam, respectively, then the directions Ox and Oy define a plane containing all the instrumental elements. The Oz axis is perpendicular to this plane.

The components of the total fluorescence intensity along the three coordinate axes are designated I_x, I_y and I_z. The sum of these three components is equal to the total fluorescence intensity, S.

$$S = I_x + I_y + I_z \tag{1}$$

The exciting beam may correspond to either unpolarized, or natural, light or to linearly polarized light whose direction of polarization is along the Ox or Oz axis. In the case of unpolarized light, the electric vector may have any orientation within the x-z plane. Symmetry considerations therefore require that

$$I_x = I_z \tag{2}$$

so that the total intensity, from eq. 1, is given by

$$S = 2I_z + I_y \tag{3}$$

When the exciting beam is polarized along the Oz axis, symmetry now dictates that

$$I_x = I_y \tag{4}$$

and

$$S = I_z + 2I_y \tag{5}$$

Finally, if the exciting beam is linearly polarized along the Ox axis, we have

$$I_y = I_z \tag{6}$$

and

$$S = 2I_z + I_x \tag{7}$$

It is usual to perform fluorescence anisotropy measurements with an exciting beam which is polarized in the z-direction or, somewhat less commonly, with unpolarized light. For both cases, the measured quantities are the components of fluorescence intensity which are polarized in the Oz and Oy directions. (The component which is polarized in the Ox direction is not accessible to measurement, as this is the direction of observation.) In this case it is useful to define

$$I_{\parallel} = I_v = I_z \tag{8}$$

and

$$I_{\perp} = I_h = I_y \tag{9}$$

In terms of the usual laboratory arrangement, $I_{\parallel}$ and $I_{\perp}$ may be identified with the vertically (I_v) and horizontally (I_h) polarized components, respectively.

The emission anisotropy, A, is defined by

$$A = (I_{\parallel} - I_{\perp})/S = D/S \tag{10}$$

where

$$D = I_{\parallel} - I_{\perp}$$

Employing eqs. 5 and 10, we obtain, for vertically polarized exciting radiation,

$$A_v = \frac{I_{\parallel} - I_{\perp}}{I_{\parallel} + 2I_{\perp}} \tag{11}$$

and, for unpolarized exciting radiation,

$$A_u = \frac{I_{\parallel} - I_{\perp}}{2I_{\parallel} + I_{\perp}} \tag{12}$$

It may be shown that the emission anisotropies for the two cases are related by

$$A_v = 2A_u \tag{13}$$

For horizontally polarized exciting light, we have

$$I_{\parallel} = I_{\perp} \tag{14}$$

and

$$A = 0$$

If more than one fluorescent species is present, the observed anisotropy is given by [10]

$$A = \sum_i A_i f_i \tag{15}$$

where A_i and f_i denote the emission anisotropy of species i and its fractional contribution to the total intensity, respectively.

2.2. Time decay of anisotropy

The measurement of fluorescence anisotropy depends upon the selective and nonrandom excitation of fluorescent molecules or groups. When a fluorophore absorbs a quantum of radiant energy, it undergoes a transition to some vibrational level of a higher electronic state [9]. This is followed by a very rapid (several picoseconds) process of internal conversion which places the fluorophore in a low vibrational level of the lowest electronic excited state. This process generally attains completion prior to the emission of fluorescence. It results in a nonequivalence of the transition moments corresponding to absorption and emission [2–4].

For the case of common interest where absorption and emission are strongly permitted electronic transitions and the wavelengths of measurement correspond fairly closely to the 0–0 vibronic transition, the transition moments of absorption and emission may be represented as linear with a well-defined direction [2]. If λ is the angle between the two linear oscillators, then A_0, the anisotropy of the immobilized fluorophore, is given by:

$$A_0 = (3\cos^2\lambda - 1)/5 \tag{16}$$

A fluorophore is excited with a probability which is proportional to $\cos^2\phi$, where ϕ is the angle between the absorption transition moment and the electric vector of the exciting beam. If the exciting beam is vertically polarized, preferential excitation will occur of those molecules whose transition moments are oriented in the z-direction. For unpolarized exciting radiation, those molecules whose moments lie in the xz plane are preferentially excited.

For short times after excitation, before significant Brownian rotation has occurred, the relative magnitudes of $i_{\parallel}$ and $i_{\perp}$ reflect this biased distribution. However, because of the finite breadth of the excitation pulse, Brownian rotation occurs while excitation is still taking place, so that the maximum observed value of A is less than the true value of A_0.

For a fluorophore with rotational mobility in a liquid medium, the direction of the transition moments becomes progressively randomized with time until a uniform distribution is ultimately approached with $i_{\parallel} = i_{\perp}$ and $A = 0$. Therefore, the time dependence of the anisotropy, $A(t)$, will be described by a sum of exponential functions, corresponding to the various rotational modes of the particles, of the general form

$$A(t) = \sum_i a_i \exp(-6D_i t) \tag{17}$$

where a_i are the preexponentials, i.e., the initial anisotropies corresponding to the various rotations, and D_i represents the rotational diffusion rates of the i-th rotational mode.

The time profile of anisotropy decay of a fluorophore is dependent upon its rate of rotational diffusion. This is in turn related to its molecular characteristics and, in the case of a fluorescent conjugate, to those of the biopolymer to which it is linked. Most commonly, one is interested in the behavior of a fluorescent probe joined covalently, or noncovalently, to a larger macromolecule. In order to obtain a manageable expression for the time dependence of anisotropy, it is necessary to approximate the actual, somewhat irregular, shape of the macromolecule by a smoothed geometrical form, as an ellipsoid of revolution.

2.3. Rotational diffusion of rigid ellipsoids of revolution

The rate of rotational diffusion may be characterized by a rotational diffusion coefficient, which is analogous to the familiar translational diffusion coefficient.

In the case of a spherical particle, the rotational diffusion coefficient, D_0, is given by

$$D_0 = kT/6\eta V \tag{18}$$

where k is Boltzmann's constant, T the absolute temperature, η the solvent viscosity and V the effective hydrodynamic volume, being equal to the anhydrous volume plus an increment corresponding to the bound water of hydration.

An ellipsoid has three principal axes, each of which is associated with a characteristic rotational diffusion coefficient. The three diffusion coefficients are designated D_1, D_2 and D_3, where the subscript indicates the axis about which diffusion occurs. In the case of a symmetrical ellipsoid of revolution, if axis 1 corresponds to the axis of symmetry and axes 2 and 3 to the (equivalent) equatorial axes, then $D_2 = D_3$.

The rotational diffusion coefficients, D_1 and D_2, for rotation about the axis of symmetry and the equatorial axes, respectively, may be related by the following expressions to the axial ratio of the ellipsoid, γ, and to the rotational diffusion coefficient, D_0, of the equivalent sphere, for a prolate ellipsoid of revolution [13]:

$$\frac{D_2}{D_0} = \frac{3}{2}\gamma\frac{[(2\gamma^2-1)\beta-\gamma]}{(\gamma^4-1)}$$
$$\frac{D_1}{D_0} = \frac{3}{2}\frac{\gamma(\gamma-\beta)}{(\gamma^2-1)} \tag{19}$$

where $\beta = (\gamma^2-1)^{-1/2}\ln[\gamma+(\gamma^2-1)^{1/2}]$.

2.4. Rotational diffusion rates and rotational correlation times

It is also useful to define a set of three rotational correlation times, σ_i, which are functions of the rotational diffusion coefficients [13,14]:

$$\sigma_1 = 1/6D_2$$
$$\sigma_2 = 1/(5D_2 + D_1) \tag{20}$$
$$\sigma_3 = 1/(2D_2 + 4D_1)$$

For a particle with spherical symmetry,

$$\sigma_1 = \sigma_2 = \sigma_3 = \sigma_0 = 1/6D_0 \tag{21}$$

Introducing the value of D_0,

$$\sigma_0 = \eta V/kT \tag{22}$$

2.5. Influence of absorption and emission transition moments on the anisotropy decay of ellipsoidal particles

We have seen how the shape of the ellipsoid regulates the rotational diffusion of the particle. Belford et al. [15] have investigated the anisotropy decay of ellipsoids of revolution, in relation to the relative positions of the transition moments and of the axes of rotations. These parameters determine the initial anisotropy (i.e., the preexponential) of the decay.

The model used by Belford et al. [15] assumes that the fluorophore is immobilized with respect to the particle, so that its transition moments have well-defined orientations with respect to the axes of the particle. The time decay of anisotropy is in this case governed by the magnitudes of the three rotational diffusion coefficients (D_1, D_2 and D_3) corresponding to the three axes and by the directions of the linear transition moments of absorption and emission.

In the limiting case of a particle with spherical symmetry, for which $D_1 = D_2 = D_3 = D_0$, the time-dependent anisotropy $A(t)$ is

$$A(t) = A_0 \exp(-t/\sigma_0) \tag{23}$$

where the quantity σ_0 is the correlation time, as described above, related to the rotational diffusion rate by

$$\sigma_0 = 1/6D_0 = \eta V/kT$$

For a symmetrical ellipsoid of revolution the governing equation is:

$$A(t) = A_1 \exp(-t/\sigma_1) + A_2 \exp(-t/\sigma_2) + A_3 \exp(-t/\sigma_3) \tag{24}$$

Here

$$\sigma_1 = 1/6D_2$$
$$\sigma_2 = 1/(5D_2 + D_1) \tag{25}$$
$$\sigma_3 = 1/(2D_2 + 4D_1)$$

where D_1 and D_2 denote the rotational diffusion coefficients for rotation about the axis of symmetry and about either equatorial axis, respectively.

and

$$A_1 = 0.1(3\cos^2\theta_1 - 1)(3\cos^2\theta_2 - 1)$$
$$A_2 = 0.3 \sin 2\theta_1 \sin 2\theta_2 \cos\phi \tag{26}$$
$$A_3 = 0.3 \sin^2\theta_1 \sin^2\theta_2(\cos^2\phi - \sin^2\phi)$$

where θ_1 and θ_2 represent the angles formed by the absorption and emission transition moments, respectively, with the axis of symmetry of the ellipsoid and ϕ is the angle formed by the projections of the two moments in the plane perpendicular to the axis of symmetry.

While, in principle, eqs. 24 and 26 would permit the estimation of the shape parameters of a rigid asymmetric protein whose shape can be reasonably approximated by an ellipsoid, in practice instrumental limitations normally make it difficult to monitor anisotropy decay over much more than one decade. This is insufficient for the accurate detection of multiple correlation times arising solely from molecular asymmetry. Further improvements in instrumentation will probably be required before these relations can be profitably capitalized on.

2.6. Influence of internal rotation

For real biopolymer systems, an intrinsic or extrinsic fluorescent label which is rigidly integrated into the three-dimensional structure, so as to have a fixed and well-defined orientation with respect to the coordinate axes of the particle, is often not obtained. In many cases, some form of internal rotation is present, so that a rotational motion of the label is superimposed upon that of the entire particle [16–18]. The various types of internal rotation which are possible may be roughly grouped into the following categories:

(1) Rotation of the fluorophore about the bond linking it to the biopolymer;

(2) Rotational wobble of that portion of the biopolymer in proximity to the fluorophore;

(3) Rotation of a well-defined molecular domain as a unit about a flexible hinge point.

In practice, more than one rotational mode may be simultaneously present.

The complexity of the general problem does not favor the development of a comprehensive theory which would encompass a wide range of cases. In particular, the data obtainable with the current instrumentation do not readily lend themselves to analysis in terms of the more general theoretical treatments, especially if more than one internal rotational mode is present [35]. However, it is possible to obtain tractable solutions for several special cases of interest.

For the case of a probe, assumed to possess cylindrical symmetry, which is linked to a larger particle, it is possible to obtain relatively simple expressions which account for the effects of the rotational wobble of the probe, provided that either the transition moment of absorption or that of emission is aligned parallel to the axis of symmetry. For a model of this kind, the symmetry axis of the probe is represented as diffusing freely within a cone of semi-angle Ξ_0. In this case the time decay of anisotropy is given by the following expression for a spherical particle [18–20]:

$$A(t)/A_0 = g\exp(-t/\sigma) + (1-g)\exp\{-t(\sigma^{-1}+\sigma_e^{-1})\} \quad (27)$$

where σ and σ_e are the correlation times corresponding to the global rotational motion of the particle and the effective correlation time of the label, respectively *, and g is the fractional contribution of the global motion.

If $\sigma_e \ll \sigma$, then eq. 27 may be rewritten in the approximate form:

$$A(t) = a_1\exp(-t/\sigma) + a_2\exp(-t/\sigma_e) \quad (28)$$

where the sum of $a_1 + a_2$ is equal to A_0, the anisotropy at zero time.

Eq. 28 has been widely used as an empirical relationship to describe the anisotropy decay of labeled macromolecules when more than one rotational mode is present. Two rotational modes is probably the practical limit which can usually be distinguished with current instrumentation and analytical procedures. Of course, it is not usually feasible to determine the orientation of the transition moments with respect to the axis of the effective rotating unit containing the probe and thus it is not normally possible to assign an unambiguous meaning to the two correlation times, except with the aid of arbitrary assumptions.

If the assumptions cited above are valid and the axis of the probe can be represented as wobbling within a cone of semi-apex angle Ξ_0, then the relative magnitudes of a_1 and a_2 may be described by [18,20]

$$\frac{a_1}{a_1+a_2} = \frac{a_1}{A_0} = \cos^2\Xi_0(1+\cos\Xi_0)^2/4 \quad (29)$$

The magnitude of Ξ_0 provides an index of the amplitude of rotational freedom of the probe. The wobbling within a cone model implies the existence of a square-well potential which restricts rotation.

An alternative model is that for which the probe rotates about a fixed axis, to which the emission transition moment makes a constant angle Ξ_0'. In this case [20],

$$\frac{a_1}{a_1+a_2} = \frac{a}{A_0} = \left\{\left(3\cos^2\Xi_0' - 1\right)/2\right\}^2 \quad (30)$$

In actual systems the existence of completely free rotation of the fluorophore is somewhat improbable and some degree of hindrance to rotation is likely to be present. It is useful to consider the limiting case where the label undergoes strongly hindered rotation. For this model the label may exist in any of several orientations corresponding to potential energy minima; the time spent in the specific positions is long in comparison with that in transit between positions. In this case the rate-limiting factor for rotation is the probability of a jump between specific orientations. The following equation was derived by Gottlieb and Wahl [16] for this model:

$$\begin{aligned} A(t) &= \exp(-t/\sigma) \\ &\quad \times\{(A_2+A_3)\exp(-Kw't) + A_1\} \\ &= \exp(-t/\sigma) \\ &\quad \times\{(A_2+A_3)\exp(-wt) + A_1\} \end{aligned} \quad (31)$$

* Eq. 27 is strictly valid only if either the absorption or the emission transition moment is parallel to the axis of the probe. If this is not the case, rotational diffusion about the axis of the probe, as well as the rotational wobble of the axis itself, can contribute to the time decay of anisotropy, so that the theory becomes considerably more complex [18,19].

where w' is the frequency of jumps between positions; K a numerical constant and $w = Kw'$.

Eq. 31 may be rewritten in a form analogous to eq. 28. The parameter σ_e now has the meaning:

$$1/\sigma_e = 1/\sigma + w \tag{32}$$

If the above model is strictly adhered to, and the conformation of the surface of the macromolecule is not modified by addition of viscosity agents like sucrose and glycerol, w should be insensitive to solvent viscosity, since it depends solely on the magnitude of the potential energy barrier encountered by a transition between different positions. This property may provide a potential means of ascertaining the validity of the model [2–4]. If the viscosity of the solvent is altered by the addition of sucrose, glycerol, or some other viscosity-increasing substance, then from eq. 27, the value of σ_e is now given by,

$$1/\sigma_e' = 1/\beta\sigma + w \tag{33}$$

where β is the factor by which the viscosity is increased. If measurements are made for a series of viscosities and $1/\sigma_e$ is linearly extrapolated vs. $1/\beta$ to $1/\beta = 0$, then the intercept and slope should yield w and $1/\sigma$, respectively. This analysis is based on the assumption that the effective microviscosity sensed by the label is equivalent to the bulk viscosity of the solvent. The rotating label may be partially, or wholly, shielded from the solvent, so that the effective microviscosity is less than the bulk viscosity. In this case, extrapolation according to eq. 33 would lead to an underestimation of $1/\sigma$ and an overestimation of w.

The above simplified models do not adequately account for the more general case where the independent motion of the probe is superimposed upon the rotational wobble of the adjacent polypeptide or the rotation of a well-defined subelement within the overall protein structure. With the usual instrumentation available today it is questionable whether more than two correlation times can be reliably extracted from anisotropy decay data. If more than two rotational modes are present, application of an equation of the form of eq. 28 will result in poorly defined averages. However, in favorable cases where the probe is firmly immobilized in the tertiary structure, the detection of a correlation time close to that expected for a well-defined molecular domain is evidence for the free rotation of the domain.

2.7. *Effects of the joints on segmental motion*

Wagener et al. [21] have estimated the effect of flexible joints on the rotational behavior of protein segments. The limits of these estimations are represented by complete flexibility and complete rigidity of the joints. In a protein constituted by two spherical segments of equal size, the presence of the joint decreases the rotational diffusion rate of the free segments by 1.3–3.5-fold between the two limits. If the segments are very long prolate ellipsoids or cylinders the decrease is between 1.7- and 8-fold. If the segments are unequal the smaller segment is more affected than the larger one, within the same limits. Limitation of the *translational* mobility plays a major role in prolonging the correlation times in the case of universally flexible joints.

Rotations about the major axis of symmetry are little affected by the presence of a flexible joint.

2.8. *Measurements of the time-dependent anisotropy*

The observable is the decay of emission intensity after excitation. The decay is either directly measured by following in the dark the time dependence of the emitted intensity after short flashes of light (time domain), or inferred by comparing the sinusoidal shape of the modulation of emitted light with that of the incident light (frequency domain). Lifetimes measured with parallel and perpendicularly oriented polarizers in excitation and emission allow estimation of the time dependence of the anisotropy of the emitted light, based on eqs. 1–15.

The numerical values of the correlation times which describe the decay are estimated by curve-fitting procedures based on the various model equations which are assumed to describe the phenomenon. Eq. 17 is in practice the most widely used numerical model, substituting correlation times σ_i for the rotational diffusion rates, as discussed in section 2.4.

It should be stressed that all of the models proposed above for interpreting the meaning of correlation times can be expressed by a sum of exponentials. Constant terms in the sum are produced by correlation times having an infinite value. This occurs when the correlation time is much longer than the lifetime of the probe so that the depolarization produced by that component cannot be detected during the span of the intensity decay.

The details of the various numerical procedures and the statistical evaluation of goodness of fit are not within the scope of this review. The reader is referred to specialized publications [3,4,6].

3. Estimation of rotational correlation times

In systems endowed with internal flexibility the librations of the various segments will interfere with each other according to the nature of the joints which keep them together. The equations which describe the depolarization produced by the various rotating units will be essentially of two kinds. For the case of universally flexible joints (so defined that they affect only the translational mobility of the particles) a sum of exponentials will be the decay law as in

$$A(t) = \sum_i A_0 [f_i \exp(-t/\sigma_i)] \tag{34}$$

where A_0 is the initial anisotropy of the system and the f_i denote the fractional depolarizations produced by the various rotations.

For rigid joints, where the librations of the segments compound with each other, a product of exponentials will be more appropriate for describing the decay as in [16]:

$$A(t) = A_0 \Pi_i [\exp(-t/\sigma_i)] \tag{35}$$

It should be stressed that eq. 35 can be transformed into a single exponential function. Therefore mixed situations will result in sums of exponentials where some of the terms may originate from products as in eq. 35 [16].

Thus, the effect of the various parameters, which according to theory are affecting the decays, will always be averaged by a sum of exponentials that are very difficult to partition among the original parameters, unless they can be independently measured.

This implies that, with the resolution currently available, anisotropy decay can hardly be used for measuring individual molecular parameters of macromolecules. Nevertheless, relevant information can be obtained on a comparative basis, with regard to internal flexibility of proteins and conformational changes of allosteric systems.

The basis of these investigations is the estimation of the correlation time associated with the macromolecule as a rigid rotor. Departures from these anticipations would indicate either the presence of polymers, for longer correlation times, or the existence of internal flexibility, for shorter correlation times.

The classic equation (eq. 22) which relates the correlation time of a molecule with its spherical volume is

$$\sigma_0 = \frac{V\eta}{kT} \tag{36}$$

where V (in cm^3) is the volume of the molecule, η the viscosity of the solvent (in P), k (in erg deg^{-1} mol^{-1}) Boltzmann's constant, and T the temperature (in K). The parameter V is related to the molecular weight and the hydration of the molecule by

$$V = \frac{M(v+h)}{N} \tag{37}$$

where M represents the molecular weight (in g), v the partial specific hydration volume of the molecule (in cm^3/g) and h the volume (in cm^3 water per g protein).

Yguerabide [13] has compared the values of σ estimated for the nonhydrated sphere by eq. 36 with the experimental values obtained for several proteins, whose anisotropy decay was monoexponential. The observed correlation times were in all cases larger than those anticipated from eq. 36. The ratios $\sigma_{obs}/\sigma_{cal}$ were near 2 with a minimum of 1.4 and a maximum of 2.4. The discrepancy could not be imputed solely to the hydration parameter, because it would have required hydrations as large as 1 cm^3/g or more. The shape of

the molecule is clearly playing a role in prolonging the single detectable correlation time.

This is the origin of the conventional rule of thumb that the equivalent spherical rotor of a protein has a correlation time nearly double that computed with eq. 36 with no hydration volume, i.e., 0.8 ± 0.1 ns/kDa.

A better approach is to use sedimentation velocity data for estimating the effective radius, and hence the effective volume, of the molecule in solution. In fact sedimentation velocity depends on the molecular weight and time-averaged hydrodynamic parameters of the protein.

By combining the equation of Stokes' law with those describing the sedimentation velocity it is possible to derive the expression

$$r_e = \frac{M(1 - v\rho_0)}{6N\pi\eta s} \tag{38}$$

where r_e is the effective radius (in cm), ρ_0 the density of the solvent, s the sedimentation velocity (in s) of the system, v the partial specific volume of the protein and η the viscosity of the solvent. From this the effective volume of the molecule can be estimated, and hence its correlation time from eq. 36. This procedure requires the independent measurement of sedimentation velocity. The measurement is not difficult, and data are available for several systems.

Table 1 shows how data obtained from variously hydrated spherical models, and from the sedimentation constants, compare with correlation times experimentally obtained by various authors.

Clearly, the sedimentation data provide a reliable basis for the estimation of the expected correlation times of entire molecules.

4. Anisotropy decay of intrinsic biopolymer fluorophores

4.1. Anisotropy decay of a rigid protein: Staphylococcus aureus nuclease

Staphylococcus aureus nuclease B, whose molecular weight is 2.0×10^4, contains a single tryptophan residue. Time-domain measurements of its anisotropy decay were made in an early study by Munro et al. [5] which employed a synchrotron light pulse as the excitation source. The half-width of this source, 0.65 ns, was substantially less than those of the flashlamps in common use at that time and facilitated the detection of very rapid rotational modes.

The time decay of fluorescence intensity at pH 7.4 and 20 °C was found to be exponential, corresponding to a single decay time of 5.05 ns. The time decay of anisotropy was also found to be

Table 1

Estimation of rotational correlation times of proteins from their molecular parameters

Eq. 36 was used in conjunction with eq. 37 for computing the correlation times of the variously hydrated spheres. Eqs. 36 and 38 were used for computing the correlation times using the sedimentation velocity data. The last column on the right lists the experimental values reported for the correlation times of the various systems. The data are corrected for the viscosity of water at 20 °C.

Protein	Molecular parameters			Correlation times (ns)					
	Molecular mass (Da)	v (cm^3/g)	s (s)($\times 10^{-13}$)	Based on hydration (in cm^3/g)				Based on sedimentation velocity	Observed
				0.0	0.3	0.6	0.9		
Apomyoglobin	16800	0.741	2.04	4.6	6.4	8.3	10.1	8.4	8.3 [a]
Trypsin	23500	0.737	2.48	6.3	8.9	11.5	14.1	13.3	12.9 [b]
Chymotrypsin	23200	0.721	2.54	6.1	8.7	11.2	13.8	14.2	15.1 [c]
Carbonic anhydrase	30600	0.740	3.30	8.3	11.6	15.07	18.4	12.0	11.2 [b]
Serum albumin	66000	0.733	4.60	17.6	25.0	32.3	39.5	48.2	41.7 [d]
Fibrinogen	340000	0.71	7.90	88.6	126.1	163.5	200.9	1600.0	1200.0 [e]

[a] From ref. 22; [b] ref. 23; [c] ref. 24; [d] ref. 25; [e] ref. 26.

exponential and could be described in terms of a single rotational mode, of correlation time 9.85 ns. Thus, no evidence for any internal rotational modes was found in this study.

Lakowicz et al. [27] have subsequently reinvestigated this system, employing frequency-domain measurements. In contrast to the earlier study, two decay components were required for an optimal fit of the fluorescence intensity decay, with α_1, $\alpha_2 = 0.68$, 0.32 and τ_1, $\tau_2 = 4.60$ and 7.31 ns, respectively.

The time decay of fluorescence anisotropy was also biexponential, with a_1, $a_2 = 0.018$, 0.301 and σ_1, $\sigma_2 = 0.091$ and 10.2 ns, respectively. The contribution of the more rapid rotational mode, although minor, appeared to be real, in view of a 2-fold decrease in χ^2 over the one-component fit.

The model which emerges from these studies depicts the tryptophan as sensing a relatively rigid microenvironment, in which its rotational motion is confined to a rather narrow cone. Both studies assign a correlation time near 10 ns to the dominant rotational mode. The correlation time predicted for a rigid hydrated sphere of the molecular weight of *S. aureus* nuclease, assuming a hydration of 0.2, is 7.6 ns. The somewhat larger value observed can easily be attributed to the contribution of molecular asymmetry.

S. aureus nuclease thus provides an example of a protein with only slight mobility of its intrinsic fluorophore.

4.2. Rotational dynamics of flexible polypeptides: adrenocorticotropin and melittin

An example of the application of fluorescence anisotropy decay to a small polypeptide with internal flexibility is provided by the time-domain study by Ross et al. [28] upon adrenocorticotropin-(1–24) (ACTH). The fluorescence of the single tryptophan group of ACTH, Trp-9, was examined. The time decay of fluorescence intensity could not be adequately fitted by a single-exponential decay law. The assumption of at least two decay times was required to yield an acceptable fit; no further improvement occurred if three components were assumed. Two decay components were found in the absence and presence of 20% sucrose and at temperatures ranging from 3.5 to 15 °C (table 2).

Since only one tryptophan is present, heterogeneity can be ruled out as a source of the multiple decay components; as the decay times were independent of emission wavelength, it is also unlikely that a two-state excited-state reaction is responsible. The most plausible explanation is

Table 2

Fluorescence lifetime (a) and fluorescence anisotropy (b) parameters of ACTH

Method A: time-domain [28]. The excitation wavelength was 295 nm. The data are the average of determinations of 340, 360, 380 and 400 nm. Method B: frequency-domain [27].

	Method	Solvent	T (°C)	η (cP)	α_1 or a_1	τ_1 or σ_1 (ns)	α_2 or a_2	τ_2 or σ_2 (ns)
(a)	A	0.1 M phosphate (pH 7.0)	3.5		0.59 ± 0.02	2.31 ± 0.03	0.41 ± 0.02	5.93 ± 0.09
	A	0.1 M phosphate (pH 7.0)	10.0		0.57 ± 0.03	2.03 ± 0.07	0.43 ± 0.03	5.13 ± 0.11
	A	+20% sucrose	3.5		0.02 ± 0.01	2.32 ± 0.02	0.38 ± 0.01	6.03 ± 0.05
	A	+20% sucrose	10.0		0.67 ± 0.01	1.97 ± 0.06	0.34 ± 0.02	5.70 ± 0.04
	A	+20% sucrose	15.0		0.66 ± 0.02	1.97 ± 0.06	0.34 ± 0.02	5.05 ± 0.09
	B	0.1 M phosphate (pH 7)	20.0		0.53	1.14	0.47	3.62
(b)	A	0.1 M phosphate (pH 7.0)	3.5	1.65	0.13 ± 0.04	0.92 ± 0.08	0.05 ± 0.01	4.47 ± 1.47
	A	+20% sucrose	3.5	3.32	0.12 ± 0.01	0.73 ± 0.04	0.08 ± 0.01	13.13 ± 1.08
	A	+20% sucrose	10.0	2.65	0.13 ± 0.02	0.69 ± 0.10	0.07 ± 0.01	6.19 ± 1.19
	A	+20% sucrose	15.0	2.27	0.12 ± 0.01	0.73 ± 0.05	0.07 ± 0.01	4.94 ± 0.73
	B	0.1 M phosphate (pH 7)	20	1.00	0.19	0.20	0.12	1.80

in terms of a mobile tryptophan group which can sample different microenvironments by rotation. Contact with different amino acid side chains may result in different degrees of quenching of the indole excited state and hence in multiple lifetimes.

This model was supported by measurements of the time decay of anisotropy. For all conditions examined, a satisfactory fit was obtained only with the assumption of two rotational modes (table 2). The more rapid rotational mode corresponded to a correlation time in the subnanosecond range and was attributed to a localized motion of the tryptophan. The magnitude of the shorter correlation time was almost independent of viscosity. The longer correlation time, which was viscosity-dependent, had a magnitude roughly consistent with rotation of the entire molecule.

The failure of the more rapid rotational mode to respond to an alteration in viscosity is not unexpected if the rotation of the tryptophan involves a transition between different potential energy minima and the rate-limiting step is the probability of release from a position of minimum energy. Alternatively, if the tryptophan rotates freely within a cone, the solvent composition and effective viscosity in its vicinity may be different from those of the bulk solution.

Lakowicz et al. [27] have subsequently reexamined the ACTH system using frequency-domain measurements. There was qualitative agreement with the time-domain results in that the time decays of both fluorescence intensity and anisotropy were found to be biexponential (table 2). As in the earlier study, the anisotropy decay could be described by a subnanosecond correlation time, reflecting the localized motion of the tryptophan, and a longer correlation time corresponding to the motion of all, or a major portion of, the molecule. While the values of the correlation times are smaller than those found by Ross et al. a quantitative comparison is difficult in view of the different experimental conditions.

It remains uncertain as to whether the rapid rotational mode reflects solely the motion of the tryptophan with respect to the balance of the protein, or whether neighboring residues are involved. It also remains to be seen whether only two rotational modes are strictly present, or whether additional modes may be detected with the development of techniques of higher resolution.

The amphipathic peptide melittin, which is isolated from bee venom, consists of 26 amino acids [29]. The sole aromatic chromophore is a tryptophan residue at position 19. In solution at low electrolyte concentration, melittin is believed to exist as a largely structureless monomer. At high ionic strengths, self-association occurs to form a tetrameric species, which is mostly α-helical [29].

Lakowicz et al. [30] have employed frequency-domain measurements to examine the anisotropy decay of monomeric and tetrameric melittin [30]. In each case determinations were made in the absence and presence of the quencher acrylamide. Dynamic quenching by acrylamide increases the fraction of the total emission which occurs on the subnanosecond time scale, thereby providing increased information about rotational motions in the picosecond range. This is of particular usefulness in studying the internal motions of proteins and peptides.

In 0.01 M Tris (pH 7, 20 °C) where melittin is monomeric, the intensity decay was found to be multiexponential and characterized by decay times of 0.2, 2 and 4 ns in the absence of quenching. The addition of increasing levels of acrylamide resulted in a progressive reduction of the magnitude of the decay times, which were equal to 20 ps, 260 ps, and 1.39 ns, respectively, in 2 M acrylamide.

The anisotropy decay of monomeric melittin could be analyzed acceptably in terms of two rotational modes. The corresponding correlation times were essentially independent of the degree of quenching by acrylamide, indicating that the decays of intensity and anisotropy were not coupled and that acrylamide does not modify the rotational modes. Almost 60% of the anisotropy decay was associated with the more rapid rotational mode, with a correlation time of about 160 ps, while the remainder decays with a correlation time near 1.7 ns.

In the presence of 2 M NaCl, in which melittin is tetrameric, the intensity decay was also multiexponential and required the assumption of three decay times for acceptable fitting, whose magni-

tudes decreased from 0.2, 2 and 5 ns in the absence of quencher to 0.04, 0.3 and 1.2 ns, respectively, in 2 M acrylamide.

As in the case of monomeric melittin, the anisotropy decay was biexponential. In this case the dominant rotational mode, which accounted for about two-thirds of the anisotropy decay, corresponded to a correlation time near 3.5 ns, while the balance of the anisotropy decays with a correlation time close to 60 ps.

The longer correlation times observed for both monomeric and tetrameric melittin are in the range expected for rotation of the entire molecules, to which they can probably be attributed. The more rapid rotational mode must arise from some form of internal rotation involving tryptophan. It is of interest that the correlation time associated with the more rapid rotational mode is longer for monomeric than for tetrameric melittin (160 vs. 60 ps), presumably reflecting the differing contribution of segmental motion involving tryptophan in the two cases. It is also worthy of mention that no convincing evidence was found for the presence of a correlation time of magnitude 1–2 ps, which would arise from the unhindered rotation of a single indole group.

Time-domain measurements of the anisotropy decay of melittin have been made by Tran and Beddard [31]. Their findings agree qualitatively with those of Lakowicz et al. in that short and long correlation times were observed; the magnitude of the latter was in the range expected for rotation of the entire molecule. The principal difference between the two studies was in the magnitude of the shorter correlation time for which Tran and Beddard observed a value of 600–700 ps, which was substantially larger than that reported by Lakowicz et al. An anomalously low value of 0.14 was found for A_0 for excitation at 300 nm. It is possible that the time resolution of this study was insufficient to recover the early portion of the anisotropy decay, resulting in a low value of A_0 and an elevated correlation time [30].

4.3. Anisotropy decay of a transfer RNA

The presence of a natural fluorophore, the Wye base, in the anticodon loop of several tRNA species permits dynamic fluorescence measurements to be made directly upon the unmodified molecules. In an early pioneering study, Beardsley et al. [32] carried out time-domain measurements of the decay of fluorescence intensity and anisotropy for yeast $tRNA^{Phe}$.

The physical properties of $tRNA^{Phe}$ are modified by Mg^{2+} ligation, which results in changes in circular dichroism and a major increase in quantum yield of the Wye base. Beardsley et al. found that the intensity decay could be described by a single decay time of 4.3 ns, which increased to 6.3 ns in the presence of 10 mM Mg^{2+}. However, the quality of the fits was poor, as judged from the χ^2 values, suggesting the presence of unresolved multiexponential decay.

Parallel time-domain measurements of anisotropy decay were analyzed in terms of a single rotational mode. Correlation times of 9.2 and 9.8 ns were found in the absence and presence of Mg^{2+}, respectively. The predicted correlation time for a rigid anhydrous spherical molecule of the same molecular weight is about 15 ns. Since the effect of hydration, or any deviation from spherical symmetry, would be to increase the average correlation time, the above value is a lower limit. It was accordingly concluded that internal rotational modes involving the Wye base were present and that $tRNA^{Phe}$ possesses a significant degree of flexibility.

Wells and Lakowicz have recently reexamined this system by frequency-domain measurements of intensity and anisotropy decay [33]. With the improved resolution of the current instrumentation, it is evident that at least two decay times are required to fit the intensity decay (table 3). In both the absence and presence of Mg^{2+} the intensity decay could be adequately described by a short decay time of about 2 ns and a longer time near 6 ns. However, the relative contributions of the two depend on the Mg^{2+} level. In the absence of Mg^{2+} the amplitudes associated with the two decay times are approximately equal; the addition of Mg^{2+} increases the relative amplitude corresponding to the 6 ns decay time to over 5-times that for the shorter decay time.

A plausible explanation for the above observations is that the Wye base exists in two microen-

Table 3

Intensity decay times (a) and anisotropy decay (b) for the Wye base in yeast $tRNA^{Phe}$

Intensity decay times: $I(t) = \Sigma \alpha_i e^{-t/\tau_i}$. Anisotropy decay: $A(t) = \Sigma a_i e^{-t/\phi_i}$. Conditions were identical for both a and b: the solvent comprised 10 mM Tris, 100 mM KCl, 25 °C, plus either 0.5 M EDTA or 10 mM Mg^{2+}.

$[Mg^{2+}]$ (mM)	α_i or a_i	τ_i (ns)	ϕ_i (ns)	χ^2_R
(a)				
0	0.50	1.7		2.3
	0.50	5.9		
10	0.16	2.7		1.4
	0.84	6.0		
(b)				
0	0.11		0.3	1.5
	0.15		18.5	
10	0.05		0.4	0.5
	0.17		17.4	

vironments which result in different decay times. A Mg^{2+}-induced conformational change favors the microenvironment associated with the 6 ns decay time.

Anisotropy decay studies also indicated a major influence of Mg^{2+} (table 3). In both the absence and presence of Mg^{2+} the anisotropy decay could be accounted for in terms of two rotational modes, corresponding to correlation times near 18 and 0.3–0.4 ns. The presence of Mg^{2+} substantially increased the relative contribution of the slower rotational mode, which now dominated the anisotropy decay. It is probable that the longer correlation time represents the global rotation of the molecule, while the shorter value arises from a localized motion of the fluorophore. An obvious explanation is that the anticodon loop, which contains the Wye base, is somewhat flexible in the absence of Mg^{2+}, with a significant degree of mobility of the bases. The binding of Mg^{2+} constrains the anticodon loop into a relatively rigid conformation in which the mobility of the bases is substantially reduced.

5. Anisotropy decay of immunoglobulins

Anisotropy decay has played a major role in elucidating the correlation between molecular dynamics and flexibility in immunoglobulins. IgG were the first molecular systems which revealed the presence of correlation times shorter than those expected for the entire molecule; moreover, the characteristics of those correlation times appeared to be related to the biological activity of the protein [23].

It may be useful to recall that the basic structure of the immunoglobulin IgG includes two identical antigen-binding segments, Fab, connected to the remainder of the molecule, Fc, by short bridges of the polypeptide chain referred to as hinges. The Fab and Fc segments also include closely packed distinguishable domains of repetitive sequence. There are three binding sites of biological relevance on the molecule. Two are on the Fab segments, and are the antigen-binding sites, another is on the Fc portion and binds to cell receptors (staphylococcal protein A, surface of leukemia cells) and to C1q subcomponent of complement, which is in this way activated.

5.1. Flexibility of soluble immunoglobulins

The inherent flexibility of immunoglobulins had been anticipated from hydrodynamic [35], electron microscopic [36,37] and X-ray crystallographic studies [38]. Consistent with these investigations, steady-state measurements of the anisotropy of immunoglobulins had given indication of the presence of short correlation times in the system, too short to be attributed to the tumbling of the entire molecules [39]. Using time-dependent anisotropy Yguerabide et al. [23] demonstrated the presence in the IgG system of at least two correlation times which they referred to the motions of the Fab segments and of the entire molecule, respectively.

Since then numerous investigators have analyzed the time-dependent anisotropy of various immunoglobulins and the data emerging from those studies are summarized in table 4 [23,35,40–44]. In table 4, we also report the correlation times estimated for the whole molecule either from the molecular weight and hydration of the system (eq. 37) or from the available sedimentation velocity data (eq. 38).

There is a general consensus among the various authors on the qualitative aspects of the time-de-

Table 4

Correlation times of various immunoglobulin systems

The experimental values are compared to those anticipated either from hydrated spherical models, or from sedimentation velocity data. The data are corrected for the viscosity of water at 20 °C. SIgA, secretory immunoglobulins A; PYS, pyrenesulfonyl chloride.

Protein	Molecular parameters			Correlation times (ns)						
	Molecular mass (kDa)	v (cm^3/g)	s (s) ($\times 10^{-13}$)	Based on hydration (in cm^3/g)				Based on sedimentation velocity	Observed ranges	
				0.0	0.3	0.6	0.9		Single	Double
										Short / Long
IgG	145 [35]	0.74 [35]	6.7 [35]	39	55	71	87	156	75–90 [b] [40] 47–81 [b] [41]	14–18 / 85–105
PYS-IgA (monomer) [42] ANS-IgA (monomer) [42]	160	0.73	7.2	42	60	78	95	185		14 [42] / >1 000
PYS-IgA (dimer) [42] ANS-IgA (dimer) [42]	350	0.73	9.5	93	132	170	209	844		16 / >1000
PYS-SIgA [42] ANS-SIgA [42]	420	0.73	11.0	112	158	205	251	932		26 / >1000 26 / >1000
IgE [41,43]	190	0.72	8.3	50	71	92	113	198	124 [b] [41]	
IgM [a] [44]	900	0.71	19.0	251	358	464	570	2800		61–93 / 568–1000
Fab [35]	52	0.74	3.8	14	19	25	31	39	28 [b,c] [41] 26–33 [c] [23]	

[a] From steady-state measurements.
[b] Weighted average.
[c] Monoexponential decay.

pendent anisotropy of these systems, namely, that it is not monoexponential and that at least two correlation times are necessary for simulating these decays. In this respect, it did not make any difference whether the immunoglobulins were labeled with a specific fluorescent antigen or with nonspecific extrinsic probes. It also did not matter whether the immunoglobulins were polyclonal or monoclonal (here including myeloma proteins). As shown by Oi et al. [41] for monoclonal antibodies the weighted averages of the correlation times depend on the nature of the antibody molecule and not on its labeling. A quantitative agreement was present only with regard to the isolated Fab segments, which in all systems appeared to have a monoexponential decay with a correlation time near 30 ns.

The polyexponential decay is indicative of internal flexibility of the molecule and it is very tempting to assign the short component to the Fab segments and the long one to the tumbling of the entire molecule. However, as noted by Hanson and co-workers [40], the long correlation time of the IgG molecules is too short for being that of the entire molecule, unless unreasonable hydration is assumed. It is one-half to two-thirds the estimate obtained from the sedimentation velocity. They concluded that both the short and long times detectable in IgG originated from librational motion of the Fab segments, and represented the motions of the V (variable) domain where the fluorescent antigen was bound ($\sigma = 14$–18 ns), and the entire Fab segment ($\sigma = 85$–105 ns), respectively. The size of the V portion is approximately one half that of the Fab segment and is consistent with a correlation time of about one-half that of the entire free segment (see table 4). It also implies a very flexible joint between the V and C

portions of the Fab molecule. As suggested by Hanson et al. [40], the two motions of the Fab segments become detectable in the IgG moiety as separate entities by virtue of the relative rigidity of the hinge regions, which slow down the librational motion of the Fab segment as a whole [21].

Table 4 shows that the libration of the V portions is detectable within the short correlation time found in the IgA and SIgA molecules. In that case, the long correlation time (> 1000 ns) is consistent with the rotation of the entire molecule. The motions of the Fab segments were not detectable, suggesting rigidity of the hinge regions of the molecule.

As shown in table 4, IgM systems are also endowed with short and long correlation times [43]. They can be considered penta-polymers of IgG globulins and the resulting molecular weight is so large that any detectable (i.e., shorter than 800–900 ns) correlation time is indicative of flexibility within the main body of the molecule. Notable is the correlation time of 568 ns found in porcine IgM, which was obtained using steady-state techniques, which are biased in favor of the longer correlation times of the system. The shorter correlation times of 70–90 ns suggest flexibility of the Fab portions of these molecules.

Flexibility of the V regions was not detected in IgM. It is possible that the limited resolving power of the steady-state technique used for the measurements did not allow resolution of the motion.

Consistent with the hypothesis that the hinge regions have limited flexibility is the observation that in IgG systems the fractional depolarization produced by their motion is only 10–15% of the total initial anisotropy of the system. Reduction of S–S bonds between the subunits of the Fc portion of the IgG molecules increases the fractional depolarization of the Fab segments, without appreciable modification of their correlation times [45].

5.2. Flexibility of C1q complement subcomponent and of bound immunoglobulins

The C1q subcomponent of human complement is a large molecular assembly constituted by a stalk of six elongated subunits, opening at one end like a flower bouquet, so as to allow the six terminal heads to interact with the Fc portions of the IgG type of immunoglobulins. Both subunits of the Fc segments are simultaneously involved in the binding. The molecular weight of the assembly is near 450000, with a sedimentation velocity of 10.2 S. Assuming a partial specific volume of $v = 0.73$, its correlation time can be estimated to range from a minimum of 120 ns for the unhydrated sphere to 1500 ns as (more realistically) obtained using sedimentation velocity data. Upon labeling with dansyl chloride Hanson et al. [46] were able to detect a very long correlation time (> 1000 ns) preceded by a rapid motion with a correlation time of 24–26 ns. This was attributed to librational activities of the heads of the six subunits.

When dansyl-specific IgG globulins were added to the C1q subcomponent the correlation times which Hanson et al. [46] were able to extract from that very complex system for the IgG globulins were very similar to those reported in table 4 for free IgG. Only the long correlation time increased from about 100 to 148 ns. Unless the binding of the head of the C1q subcomponent to the Fc portion of the molecule has a special pivotal nature, tumbling of the entire IgG molecule is prevented by this interaction. Therefore, these data support the hypothesis that also in this case, as for the free IgG globulins, both of the detectable correlation times are due to motions of the Fab segments, and that they are affected by the binding of ligands, in this case the C1q subcomponent, to the Fc segments. The increase of 48 ns in the longer correlation time can easily be referred to a decrease of the translational diffusion produced by the anchoring, as proposed by Wegener [47].

Very similar data have been obtained with IgG bound to staphylococcal protein A and anti-Fc antibodies [48,49].

Slattery et al. [43] have used steady-state procedures for measuring the correlation times associated with monoclonal dansyl-specific IgE globulins, both free and bound to their high-affinity receptors on basophilic leukemia cells. The average correlation time of 54–65 ns increased to 74–75 ns upon binding. The data are again consistent with an internal flexibility of the protein, only slightly affected by the binding of the Fc region to a bulky, practically immobile con-

stituent.

5.3. Functional relevance of the internal flexibility of immunoglobulin

The data reported by Oi et al. [41], listed in table 4, represent an attempt to correlate flexibility and biological function of immunoglobulins. They produced monoclonal antibodies with identical anti-dansyl specificity, having however different heavy chains. They included IgG1, IgG2 and IgE antibodies. Their time-dependent anisotropy was fitted to a double-exponential function, and the average correlation time was weighted over a fractional depolarization of the two components.

As shown in table 4 (data with superscript b) the averages were consistent with data previously obtained on IgG systems and were taken as an inverse measure of the flexibility of the system. The ability of these antibodies to fix complement was directly proportional to their flexibility. The IgE molecules were the least flexible and had almost no ability to activate complement. Although a fortuitous coincidence is possible, the data strongly suggest a higher biological activity connected with the flexibility of immunoglobulins.

It should be stressed, however, that the relatively rigid IgE molecules actively bind specific cell receptors [43] and are very effective in precipitating hapten-carrying proteins [50]. This may suggest a specific role of flexibility with regard to complement interactions.

The general picture that emerges from these studies is that the anticipated flexibility of the immunoglobulins has been proven and very probably is related to their function. It must serve to adapt the molecules to the stereochemistry of the particles carrying their specific haptens. There seems to be a correlation between flexibility and complement activation. However, no clear correlation has yet been established between the affinity of either the antigen-binding sites or of the Fc-binding sites and flexibility.

6. Anisotropy decays in the actin-myosin system

Another system whose internal flexibility was anticipated on functional grounds and found experimentally using nanosecond fluorescence spectroscopy is the actin-myosin system. The sliding of the thin and thick filaments, connected by cross-bridges, had to be supported by movement of myosin segments.

It may be useful to recall that, as shown in fig. 1, myosin is a rod 1500 Å long with a diameter of 24 Å. Enzymatic digestions allowed the identification of two main portions: light meromyosin (LMM) and heavy meromyosin (HMM). HMM carries the S-1 segment, also detachable as a unit by enzymatic digestion, which is responsible for the cross-bridges that establish the interaction with the actin filament. Myosin rods are formed upon enzymatic cleavage of the S-1 fragments. S-2 frag-

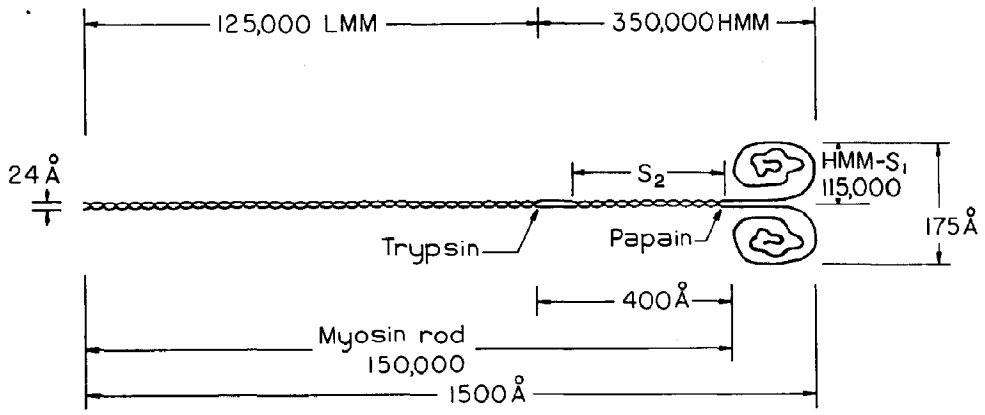

Fig. 1. Schematic representation of the myosin molecule and of the fragments which can be obtained by proteolytic digestions.

Table 5

Correlation times of the actin-myosin system

Estimation values are included based either on hydration of the spherical models, or on sedimentation velocity data. TM, tropomyosin; TN, troponin.

Protein	Molecular parameters			Correlation times (ns)					
	Molecular mass (kDa)	v (cm^3/g)	s (s) ($\times 10^{-13}$)	Based on hydration (in cm^3/g)				Based on sedimentation velocity	Observed range (single correlation times)
				0.0	0.3	0.6	0.9		
S-1 [a] [51]	115								200–250
HMM [a] [51]	350								400
LMM	173	0.73	3.25	46	65	84	103	2500	
Myosin	475	0.73	6.40	127	179	231	284	6900	440–450 [a] [51]
HMM [a] + F-actin [51]									1100–1900
Rod [b] [52]	360								−3500 (pH 8) −730 (pH 6) 184 (pH 4) 70 (pH 2)
Cross-bridges [53]	(vertical configuration)								800–1200 (relax) > 7000 (rigor)
	(horizontal configuration)								340 (relax) 300 (rigor)
F-Actin [c] [54]									650
F-Actin [c] + TM + TN [54]									760
F-Actin [c] + TM + TN + Ca [54]									409
F-Actin [d] [55]									10 s

[a] Label: IAEDANS on S-1 segment.
[b] Label: ANS or DNS; nonspecific.
[c] Label: DNS on Cys at position 357.
[d] Label: ϵ-ADP on binding site.

ments are produced by cleavage of the S-1 portions from the HMM molecules.

Only few data are available in the literature with regard to the sedimentation velocity of the system. Therefore, the estimated data in table 5 are incomplete. The $s_{20,w}$ values available for LMM and myosin provide model estimates for the other proteins.

6.1. Myosin and its cross-bridges

From the data reported in table 5 it is very suggestive that S-1-labeled HMM and myosin show practically the same correlation time, near 400 ns, while the value for isolated S-1 fragments is near 200 ns. Very probably in both cases the correlation times reflect the mobility of the S-1 portions, mobility which is slowed down by the presence of a flexible joint to the rest of the molecule [51]. This corresponds very well to the model according to which the S-1 segments of myosin form a mobile entity responsible for the formation of the cross-bridges in the myofibril, cross-bridges which should promote the sliding of the thin and thick filaments on each other. The increased correlation time of the S-1 segments when joined to the rest of the molecule is consistent with the presence of a flexible joint as anticipated by Wegener et al. [21,47].

Burghardt and Thompson [53] report very interesting data obtained for cross-bridges (actually

labeled S-1 segments) on oriented myofibrils, in both the rigor and relaxed states. The major axis of the myofibrils was either parallel (vertical) or perpendicular (horizontal) to the polarity of the incident light (vertical). The relaxed and rigor states of the fibrils were obtained by modulating the composition of the solvent in which they were immersed. Labeling was achieved by the addition of IAEDANS to the muscle fibers, a procedure which mostly labels the S-1 segments of myosin.

In the vertical configuration only the end-over-end rotation of myosin was explored. The horizontal configuration gave information on the rotational diffusion of the cross-bridges between myosin and actin. Two correlation times were detected in all cases, the short one (of a few nanoseconds) was interpreted as being due to nonspecific labeling of the muscle fibers.

In the vertical configuration the long correlation time increased from 1 μs to more than 7 μs on going from the relaxed to the rigor state, as expected from the formation of the very long and bulky assembly of actin and myosin. In the horizontal configuration the long correlation time remained near 300 ns under both relaxed and rigor conditions, and was interpreted as being due to the rotation of the cross-bridges about the major axis of the fibers.

The authors were surprised that the rigor state did not prolong the correlation time of the cross-bridges in the horizontal configuration. We are not. The detected correlation time was very consistent with the data reported by Mendelson et al. [51] on the specifically labeled S-1 segments (as reported above) and probably reflected the rotation of the cross-bridges not around the major axis of myosin, but about their own major axis. It may also indicate that the motions of the cross-bridges when the thin and thick filaments slide on each other are not synchronized. Unfortunately, no clear data have been reported on the fractional anisotropy depolarized by these librations, which might have helped in clarifying the situation.

6.2. *Isolated myosin rods*

The isolated rods of myosin, labeled with ANS or DNS, exhibit a complex behavior [52]. At neutral and alkaline pH, Harvey and Cheung [52] were able to detect only a single *negative* correlation time as long as -3500 ns, which they took to be an indication of the rigidity of the extended rod. The shorter *positive* correlation times between 70 and 184 ns found at acid pH (see table 5) were taken as an indication of proton-induced flexibility, probably about the joint between the LMM and S-2 segments. A different interpretation is possible.

Myosin is a rod 1500 Å long with a diameter of 24 Å. The rotational modes about the various axes should be resolvable in the rigid rod. Harvey and Cheung report estimations of 97 and 27 000 ns for the correlation times produced by the rotational diffusion of the rods about their main axis and the equatorial axes (end-over-end rotation), respectively. Consistent with these anticipations as reported in table 5, the sedimentation velocity of the LMM fragment (whose length is about one-half that of the rod) suggests an overall correlation time in excess of 2 μs. Thus, in the rigid molecule and utilizing fluorescent probes such as ANS, DNS and IAEDANS whose lifetime is between 10 and 20 ns, only the rotation about the main axis of the molecule should be detectable in the rigid, extended rod.

Assuming flexibility at the trypsin-sensitive region, i.e., the joint between S-2 and LMM segments, models based on a once broken rod, or on the segmental motions of Wegener et al. [21,47], would multiply by at least 2 the end-over-end correlation time of both segments in the free state. Thus, even in the presence of a universally flexible joint between the LMM and S-2 portions of the rods the end-over-end rotation would not be detectable.

It should be stressed that according to the model of Wegener et al. [21] rotations about the main axis of flexible segments are little affected by the joint to the rest of the molecule. Therefore, the failure to detect at neutral pH the rotation about the main axis of either the extended rod or the bent segments (with a correlation time near 97 ns) is somewhat surprising. It is as if at neutral pH these rotations were inhibited in the myosin rods. This can occur only if the joint between the two segments is not universally flexible, allowing bend-

ing but not torsional freedom of the two segments with respect to each other. This would synchronize the rotation about the main axis of one segment with the end-over-end rotation of the other. The explanations given by Harvey and Cheung [52] for clarifying the negative anisotropy decay of the system, based on the orientation of the transition moment of the labels, are still valid for this model.

At acid pH the joint becomes more rigid, the bending is lost, and rotations about the major axis of the molecule become detectable with correlation times between 70 and 184 ns.

The alternative model proposed here is consistent with the findings of Burke et al. [58], based on measurements of intrinsic viscosity, which propose bending of the rods at neutral pH. This new model would also give more relevance to the hypothesis proposed by Harvey and Cheung that the swinging in and out of the thin filament of the HMM portion of myosin is regulated by the absorption and release of protons produced by the metabolic activity of the system.

6.3. Actin filaments

F-Actin labeled at the binding site of ATP shows a correlation time of 10 μs, consistent with the presence of very long filaments, whose flexibility prevented the detection of rotations about the major axis of the filament [54]. When the label substitutes the cysteine at position 357, a correlation time near 600 ns appears which decreases to about 400 ns in the presence of Ca^{2+} [54]. It is as if residue 357 is situated on a special domain of the globular structure of the single actin monomer, endowed with independent librational motions. The significance of this internal flexibility with respect to the mechanics of muscular contraction is still unexplained.

7. Correlation times in globular allosteric systems: anisotropy decay in hemoglobin and myoglobin

In the preceding sections, we have seen that the monitoring of anisotropy decay was very helpful in elucidating the molecular mechanics of the behavior of immunoglobulin and myosin, whose biological activity is linked to gross morphological attributes of the protein. Large librational segments were detected and the biological functions of these proteins appeared to be dependent on the flexibility of the hinges linking the various segments together.

In globular allosteric systems the conformational changes which are at the basis of the regulation of their biological activity must be related to the harnessing of the thermal librations of these molecules, so as to produce ordered, programmed rearrangements of the various structural levels. This should also produce structural domains capable of changing their reciprocal positions, which would result in motions whose correlation times will be shorter than those expected from the molecule as a whole.

Therefore, in these systems it should also be possible to identify librational segments. A difference with the immunoglobulins and myosin is that the characteristics of the librational motions should be dependent on the presence and nature of the ligands interacting with these proteins.

Hemoglobin is the globular system which has been investigated in greatest detail at present. This may appear surprising, since the quenching of fluorescence produced by energy transfer to the heme strongly reduces the signal emerging from fluorophores whose distance is less than two molecular diameters. Still the system is attractive because of the wealth of available information with regard to its structure and conformational properties. This also allowed labeling of the system in different positions, permitting a more complete exploration of the internal motions.

Extrinsic labeling provided emission with sufficient intensity to allow measurement of correlation times in the system. Table 6 summarizes the data so obtained [34,59–63]. The table shows that the correlation times estimated from the sedimentation velocity of the various proteins corresponded to those computed for certain hydration volumes of the moieties, assuming a spherical shape and hydrations of 0.6 cm^3/g for hemoglobin, 0.8 cm^3/g for the isolated subunits and 0.9 cm^3/g for the heme-free proteins. This increasing hydration is consistent with the increased surface of the subunits and of the heme-free compounds.

Table 6

Correlation times of the various species of the hemoglobin system

Estimated values are included based either on hydration of the spherical models, or on sedimentation velocity data. All correlation times are corrected for the viscosity of water at 20 °C. The observed correlation times were corrected for their viscosity dependence (see eqs. 32 and 33). PLP, pyridoxal 5′-phosphate; Apo-, heme-free.

Protein	Fluorophore	Position	Molecular parameters			Correlation times (ns)							
			Molecular mass (kDa)	v (cm^3/g)	s (s) ($\times 10^{-13}$)	Based on hydration (in cm^3/g)				Based on sedimentation velocity	Observed ranges		
						0.0	0.3	0.6	0.9		Single	Double	
												Short	Long
HbCO [59]	IAEDANS	β93	64.5	0.749	4.45	17	24	31	39	30.1	3.3		
HbO_2 [59]	IAEDANS	β93									3.1		
Hb [59]	IAEDANS	β93									7.1		
Hb + IHP (1 mM) [59]	IAEDANS	β93									34.1		
CO β-subunit [60]	IAEDANS	β93	16.5	0.749	1.7 [a]	4	6	8	10	9.1	3.4		
[34]	IAEDANS	β112									3.0		
Apo-Hb [62]	IAEDANS	β93	32.0	0.749	2.56	8	12	15	19	19.2		0.7	15.1
[62]	FIA	β93										0.1	12.3
[62]	PLP	β1										0.9	18.2
[62]	ANS	heme pocket										0.8	20.1
Apo β-subunit [34]	IAEDANS	β93	16.0	0.749	1.7 [a]	4	6	8	9	9.1		0.8	9.8
[34]	IAEDANS	β112									3.0		
[34]	ANS	heme pocket									10.4		
	TRP	β15, β37									9.7 [b]		
Apo α-subunit [63]	IAEDANS	α104									0.4		
[63]	ANS	heme pocket									2.0		
[63]	TRP	α14										0.6 [b]	5.1–6.7 [b]

[a] Estimated for the monomeric unit from the data of the monomeric α-subunits.
[b] From static anisotropy (Perrin plots).

This internal consistency is probably due to the actual, roughly spherical shape of the proteins of the system and confirms the reliability of sedimentation velocity data for predicting the average correlation times of macromolecules, considered as rigid units.

7.1. Correlation times of IAEDANS-labeled hemoglobin and its subunits

The reagent IAEDANS was used to label the cysteines at β93 and at β112. The last position was available only in the isolated β-subunits. The α104 cysteines were not available to the probe in the native protein.

Table 6 shows that the rotational diffusion of the liganded forms of hemoglobin and its β-subunits, labeled at β93, could be accounted for by a single apparent correlation time near 3 ns. This time is much shorter than what is expected for the entire molecule for both hemoglobin and its subunits. The dominant correlation time became longer in deoxyhemoglobin, where it approached that expected for a single subunit. The rotational diffusion of the whole tetramer became evident only after addition of IHP to deoxyhemoglobin. It

should be noted that all of these times had been corrected for their viscosity dependence (eqs. 32 and 33) and therefore are independent of local motions of the extrinsic probe.

The similar correlation times detected in hemoglobin and in the isolated β-subunits suggest that the same effective domain might be responsible for the phenomenon in both proteins. The librations of the effective domain were seemingly somewhat insensitive to the interaction of the β-subunits with the partner α-chains.

With regard to size, 3 ns would be consistent with, for example, a free spherical peptide of molecular mass 4 kDa. For a segment connected to a larger protein by a flexible universal joint, the simulations of Wegener et al. predict an actual size of 2 kDa for the domain, i.e., 15–18 amino acids.

Removal of the ligand stabilized in the system a more rigid structure, the T structure of Perutz, where the joint of this domain with the balance of the protein became more rigid, so as to prolong its detectable correlation time. Addition of IHP to deoxyhemoglobin made the joint almost completely rigid, and the global motion of tetrameric hemoglobin now became detectable.

Probably the 3 ns domain near the β93 cysteine is not the only domain capable of independent motion on the surface of hemoglobin subunits. Labeling at β112 revealed in the isolated β-subunits the presence of another domain, again very small, capable of independent motions, with a correlation time near 3 ns.

This suggests that in its liganded form the rotational diffusion of the molecule is influenced by the motion of one or more small independent domains. Their librational motion in practice prevented the detection of the rotation of the molecule as a whole.

7.2. *Tryptophan fluorophores: hemoglobin and myoglobin*

The data reported in this section are based on lifetimes and not on correlation times. The reason for mentioning them is to show that fluorescence lifetimes also contain relevant information on the conformational properties of allosteric systems.

In hemoproteins energy transfer from tryptophan to heme produces a quasi-total quenching of the light emitted from the fluorophore. Only recently have laser-based, high-resolution instruments been developed which are able to detect and investigate the characteristics of the picosecond range lifetimes of the tryptophans in hemoglobin and myoglobin [64].

The search is made more difficult because the emission originating from trace amounts of impurities, probably not carrying heme and impossible to remove by the most advanced laboratory techniques, had an intensity at least equal to that produced by the heme-quenched tryptophans. The lifetimes of the heme-free impurities were in the nanosecond range, therefore, the quenched, picosecond range lifetimes were still clearly resolvable from the emission of the contaminants.

The presence of impurities has thus far made interpretation of the apparent correlation times very unclear. Still higher resolutions will be necessary for explaining the data.

Table 7 lists the lifetimes obtained by Bucci et al. [65] and by Hochstrasser and Negus [73] for different derivatives of hemoglobin and myoglobin. It appears that the picosecond lifetimes of tryptophans were sensitive to ligand binding. As proposed by Bucci et al. [65] for the deoxy- and CO derivatives, this was due to the different tilt of the heme in the heme pocket, which is produced

Table 7

Decay times in the range of the emission from hemoglobin and myoglobin

The data on hemoglobin were collected by Bucci et al. [65], using a 2 GHz frequency-resolved machine [64]. Excitation at 300 nm, emission at 365 nm, 0.05 M phosphate buffer at pH 7.0 and 4°C. The data on myoglobin were obtained by Hochstrasser and Negus [73] using time-domain procedures on a streak camera. Excitation at 273 nm, emission at 320 nm, in 0.025 M Tris buffer at pH 8.6 and 23°C; n/a, not available.

Sample	τ (ns)	(S.D.)
Oxyhemoglobin	0.016	(0.001)
Deoxyhemoglobin	0.009	(0.001)
Carbonmonoxyhemoglobin	0.027	(0.003)
Deoxymyoglobin	0.014	(n/a)
Carbonmonoxymyoglobin	0.026	(n/a)

by ligand binding [66]. For the oxy derivatives the different lifetime was due instead to the different orientation of the electric vectors of the absorption of light in the Soret region of the spectrum.

Therefore, quenching by the heme provides the investigators with a very fine tool for observing ligand-related conformational changes in the hemoglobin and myoglobin systems. Recent unpublished data from this laboratory strongly suggest that the α-β interaction in liganded derivatives affects the tilting of the heme in hemoglobin.

7.3. Anisotropy decay of a dissociating system. Correlation times of heme-free hemoglobin and myoglobin

7.3.1. Extrinsic labeling

In our laboratory we have demonstrated that, in apohemoglobin, removal of the heme results only in the collapse of the heme pocket, with no modifications of the diameters of the hemoglobin subunits [67,68].

Apohemoglobin is a dissociating system where monomers, dimers and tetramers are present. The system is predominantly dimeric, as shown by sedimentation equilibrium experiments [69]. There is evidence that the system also contains monomers and tetramers. The presence of monomers is demonstrated by the formation of hybrid polymers constituted by heme-containing and heme-free subunits when solutions of apohemoglobin are titrated with isolated subunits of hemoglobin [70]. The presence of tetramers is proven by the increase in molecular mass of the system, up to values near 50 kDa, upon addition of IHP.

Thus, the system would be expected to exhibit correlation times reflecting the presence of the three molecular species, with their relative proportions changing with protein concentration. If only one average time were detectable, it would also be concentration-dependent.

The surface of the molecule can be labeled with a variety of fluorophores at the cysteines α104, β93, β112 and at the β1 valine. Noncovalent labeling of the heme pocket with ANS allows exploration of the librational motions of a more internal portion of the molecules. Also 'internal' to the proteins are the tryptophans in positions α14, β15 and β37.

As shown in table 6, in apohemoglobin, labeling of the surface resulted in two correlation times. One was shorter than 1 ns, in a region not resolved by the pulse instrument based on a flashlamp (Edinburgh 119) used for these measurements. This correlation time could be attributed to purely local motion of the probe. The longer component reflects the rotation of the entire molecule, or of a major portion thereof.

Labeling at β93 produced correlation times intermediate between those expected for a monomer and a dimer, suggesting the presence of internal flexibility in the dimeric molecule of apohemoglobin. Labeling with PLP at β1 resulted in a correlation time very similar to what sedimentation velocity predicts for the rotation of the entire $\alpha\beta$ dimer. The longest correlation time (again consistent with the rotation of a dimer) was obtained with ANS in the heme pocket [62]. Notably, no correlation time was detectable near 3 ns as in the liganded form of hemoglobin similarly labeled with AEDANS in position β93.

These correlation times were not sensitive to 3–10-fold variations in protein concentrations. Very similar data were obtained in either Tris or phosphate buffers (0.05 M) between pH 6.5 and 7.2. The effect of addition of IHP to the labeled proteins was erratic and has not been reported in the publications.

In the isolated apo-β and apo-α-subunits, removal of the heme is known to produce aggregating systems. The data listed in table 6 refer to experimental conditions where the heme-free subunits were essentially monomeric [34,63]. Labeling at β93 and inside the heme pocket produced essentially identical correlation times, near 10 ns, as expected for a monomeric unit. The fast librational motions present in the liganded β-subunits were still detectable upon labeling the β112 cysteine with AEDANS [34].

Removal of the heme had a major effect on the structure of the isolated α-subunits. The ellipticity in the far-ultraviolet region decreased about 2/3 at all wavelengths within the 205–230 nm region, indicating a dramatic loss of helical content, and probably unfolding of the molecule. Labeling at

α104 with IAEDANS further decreased the CD signal in the ultraviolet region, and only the local motion of the probe was detectable by anisotropy decay in the system. Labeling the heme pocket with ANS resulted in a single, fast correlation time, consistent with an extensive internal unfolding of the protein [63].

7.3.2. Tryptophan fluorescence

Table 8 presents the data obtained for the emission of tryptophan residues in apohemoglobin and apomyoglobin [69]. The global motion of apomyoglobin had a correlation time shorter than that anticipated from the sedimentation velocity of monomeric hemoglobin subunits. Apohemoglobin showed correlation times corresponding to rotational diffusion intermediate between that of monomers and dimers.

While the system was not sensitive to variations in protein concentration as shown in table 8, it was sensitive to addition of IHP. The reequilibration took a long time and only after an overnight exposure to IHP did the presence of tetramers become clearly detectable. If the measurements were made immediately following the addition of IHP to the samples the correlation times remained practically unchanged.

A very interesting finding appears for the local mobility of tryptophans in apomyoglobin and apohemoglobin. In our laboratory (C. Fronticelli, E. Bucci and H. Malak, unpublished results), in apomyoglobin, with the help of high-resolution frequency-resolved instruments it was possible to measure a correlation time of 56 ps. In apohemoglobin the shortest detectable correlation time was near 400 ps. This suggests a rigidity in the

Table 8

Correlation times of tryptophans of apohemoglobin and apomyoglobin

Estimated values are also included based either on hydration of the spherical models, or on sedimentation velocity data (eq. 38). Measurements were performed in 0.05 M phosphate buffer at pH 6.5 and 4° C. All correlation times shown have been corrected for the viscosity of water at 20° C. The tryptophan residues are in positions 7 and 14 in apomyoglobin (sperm whale) and in positions α14, β15 and β37 in apohemoglobin (both human and bovine). From the data reported in table 6 it can be inferred that, for the entire molecules, the correlation times corresponding to the sedimentation velocity of the various polymers are 9, 18 and 36 ns for the monomers, dimers and tetramers, respectively. The data shown in parentheses are below the limits of the time-resolving power of the instrument used for measurement, which for the Edinburgh 119 ns fluorometer (time resolution) was estimated to be 1 ns.

Protein	Method	Excitation wavelength (nm)	[Protein] (mg/ml)	[IHP] (mM)	Initial anisotropy (fraction	Correlation time (ns)
Apomyoglobin	time	295	1.9	–	0.24	(0.360)
					0.76	7.920
	frequency	300	1.9	–	0.24	0.056
					0.76	7.480
Apohemoglobin	time	296	0.3	–	0.12	(0.283)
					0.88	15.070
			3.5	–	0.10	(1.500)
					0.90	14.333
			2.4	1.0	0.11	(0.443)
					0.11	10.660
					0.78	21.500
	frequency	296	0.3	–	0.25	0.660
					0.75	16.110
			3.5	–	0.23	0.405
					0.77	16.670
			2.4	1.0	0.10	0.443
					0.02	32.860
					0.88	39.420

protein structure around the tryptophans that is much more pronounced in the hemoglobin system than in that of myoglobin. The question arises as to whether this different behavior is related to the allosteric properties and subunit interactions of hemoglobin, which are absent in myoglobin.

7.4. Significance of the data

The exploration of molecular dynamics of allosteric systems by time-resolved fluorescence spectroscopy is a relatively new field of investigation. Therefore, the general conclusions which we will try to extract from the experiments reported above are tentative and still await support emerging either from further investigations of the hemoglobin system or from evidence obtained for other allosteric proteins.

In hemoglobin, the disappearance of the 3 ns correlation times upon removal of the heme suggests that introduction of the heme into the heme pocket may enhance the thermal motions of the apoproteins and result in the appearance of fast-moving independent domains. This is consistent with the findings of Franchi et al. [71], based on CD data, which indicate in the β-subunits the presence of a heme-linked structural domain.

The thermal motions appear most evident in liganded hemoglobin, in the sense that the joints between the various domains are flexible enough so as to allow the detection of short correlation times. These joints become more rigid in deoxyhemoglobin, consistent with the lower energy level of the T structure, stabilized internally by salt bridges and other intersubunit interactions [72]. This view suggests that the structure of liganded hemoglobin may be less stable than that of deoxyhemoglobin. It is the energy of the heme-ligand interaction that produces the energy well in which liganded hemoglobin finds its equilibrium.

In apohemoglobin the collapse of the heme pocket and the newly established hydrophobic interaction among the groups lining the pocket add rigidity to the individual subunits. The 3 ns domains disappear, or become less readily detectable, in favor of longer correlation times consistent with the motions of entire subunits. Nevertheless, the system remains endowed with a flexibility which probably originates from a large degree of freedom at the subunit interfaces. It appears that the heme, while destabilizing the internal rigidity of the individual subunits, stabilizes the subunit interfaces, decreasing their degree of freedom.

As is evident from the data presented in table 6 the correlation times of labeled apohemoglobin were probe-dependent. They did not exceed those expected from a dimer in the samples labeled inside the heme pocket with ANS, and were as low as those expected from a monomeric hemoglobin subunit for samples labeled at β93 with FIA. The increase of the correlation time of apohemoglobin subunits from 9 ns, as expected from a monomeric unit, to 12 ns (as in the FIA-labeled protein) can easily be attributed to the presence of a flexible universal joint between spherical segments, as anticipated by Wegener et al. [21,47].

Also, the correlation times referred to the global motion of the protein were independent of protein concentration and sensitive to addition of IHP, which promotes the formation of tetramers [69], only after being allowed to stand overnight in the cold. Chu and Bucci [69] did not observe this time dependence in their experiments on sedimentation velocity. This suggests that while the polymerization is fast, the rearrangement of the subunits' conformation in order to acquire a higher rigidity is very slow.

All of the systems discussed in this review showed probe dependence of their correlation times. Their common characteristic is the presence of internal flexibility of the molecules. As predicted by eq. 35, when the multiple rotations of a macromolecule compound each other, resolution of individual correlation times becomes very difficult. Single exponential functions may perfectly describe the decay of anisotropy produced by a multiplicity of individual librations. However, the relative positions of the axis of rotation and of the transition moments regulate the fractional anisotropy of each rotational mode. For this reason it is not surprising that different probes will produce a different weighting of the depolarization arising from the various rotational modes, therefore influencing the average correlation times detectable in the experiments.

Other factors may play a role in weighting the rotational parameters. It should be stressed that time-resolved procedures base their estimation of decay functions on the preexponentials. Instead, the frequency-resolved methods base their estimation on the relative intensities of the various components (i.e., the integral of the preexponential on the decay time). On this basis it should be expected that a heterogeneous system will show different average correlation times when measured with the two techniques.

The flexibility of apohemoglobin at the subunits' interface is the origin of the probe dependence of its correlation times. It is consistent with the presence of a multiplicity of discrete polymers, whose librational motions are differently weighted by the spectral characteristics of the various probes, and by their position on the molecule, relative to the main axis of rotation of the librating segment. This may also explain the reluctance of the system to respond to protein concentration (at least within the limits of our tests).

Further investigations on different systems will reveal whether these phenomena are general characteristics of allosteric proteins, or peculiar to the hemoglobin system.

References

1 J. Monod, J.B. Wyman and J.P. Changeaux, J. Mol. Biol. 12 (1965) 88.
2 P. Wahl, in: Biochemical fluorescence, eds. R.F. Chen and H. Edelhoch (Plenum, New York, 1975) vol. 1, p. 1.
3 R.F. Steiner, Excited states of biopolymers (Plenum, New York, 1983) p. 117.
4 J.R. Lakowicz, Principles of fluorescence spectroscopy (Plenum, New York, 1983) p. 155.
5 I. Munro, I. Pecht and L. Stryer, Proc. Natl. Acad. Sci. U.S.A. 76 (1979) 56.
6 I. Isenberg, in: Biochemical fluorescence, eds. R.F. Chen, and H. Edelhoch (Plenum, New York, 1975) vol. 1, p. 43.
7 V.J. Koester and R.M. Dowben, Rev. Sci. Instrum. 49 (1978) 1186.
8 W.R. Ware, in: Creation and detection of the excited states, ed. A.A. Lamola (Marcel Dekker, New York, 1971) p. 213.
9 A. Jablonski, Z. Phys., 94 (1935) 38.
10 P. Soleillet, Ann. Phys. (Paris) 12 (1929) 23.
11 P. Wahl, G. Meyer and J. Parrod, Eur. Polym. J. 6 (1970) 585.
12 R. Memming, Z. Phys. Chem., 28 (1961) 168.
13 J.Y. Yguerabide, Methods Enzymol. 26 C (1972) 498.
14 T. Tao, Biopolymers 8 (1969) 609.
15 C.G. Belford, R.L. Belford and G. Weber, Proc. Natl. Acad. Sci. U.S.A. 69 (1972) 1392.
16 Y. Gottlieb and P. Wahl, J. Chim. Phys. 60 (1963) 849.
17 R.D. Dale and J. Eisinger, Biopolymers 13 (1974) 1573.
18 G. Lipari and A. Szabo, Biophys. J. 30 (1980) 439.
19 A. Szabo, J. Chem. Phys. 81 (1984) 150.
20 K. Kinosita, S. Kawato and A. Ikegami, Biophys. J. 20 (1977) 289.
21 W.A. Wegener, R.M. Dowben and V.J. Koester, J. Chem. Phys. 15 (1980) 4086.
22 T. Tao, Biopolymers 8, (1969) 609.
23 J. Yguerabide, H.F. Epstein and L. Stryer, J. Mol. Biol. 51 (1970) 573.
24 L. Stryer, Science 161 (1968) 526.
25 P. Wahl, C.R. Acad. Sci. Ser. D 263 (1966) 1525.
26 A.U. Acuna, J. Gonzalez-Rodriguez, M.P. Lillo and K. Razi Naqvi, Biophys. Chem. 26 (1987) 63.
27 J.R. Lakowicz, I. Gryczynski, H. Szmacinski, H. Cherek and N. Joshi, Biochemistry (1988) submitted.
28 J.B.A. Ross, K.W. Rousslang and L. Brand, Biochemistry 20 (1981) 4361.
29 T.C. Terwillinger and D. Eisenberg, J. Biol. Chem. 257 (1982) 6016.
30 J.R. Lakowicz, H. Cherek, I. Gryczynski, N. Joshi and M.L. Johnson, Biophys. J. 51 (1987) 755.
31 C.D. Tran and G.S. Beddard, Eur. J. Biochem. 13 (1985) 59.
32 K. Beardsley, T. Tao and C.R. Cantor, Biochemistry 9 (1970) 3524.
33 B.D. Wells and J.R. Lakowicz, Biophys. Chem. 26 (1987) 39.
34 J. Oton, E. Bucci, R.F. Steiner, C. Fronticelli, D. Franchi, J.X. Montemarano and A. Martinez, J. Biol. Chem. 256 (1981) 7248.
35 M.E. Noelken, C.A. Nelson, C.E. Buckley and C. Tanford, J. Biol. Chem. 240 (1965) 218.
36 R.C. Valentine and N.M. Green, J. Mol. Biol. 27 (1967) 615.
37 A. Feinstein and A.J. Rowe, Nature 205 (1975) 147.
38 L.M. Amel and R.J. Poljak, Annu. Rev. Biochem. 48 (1979) 961.
39 R. Cathou, Compreh. Immun. 5 (1978) 37.
40 C. Hanson, J. Yguerabide and V.N. Schumaker, Biochemistry 20 (1981) 6842.
41 V.T. Oi, T.M. Vuong, R. Hardy, J. Reidler, J. Dangl, L.A. Herenberg and L. Stryer, Nature 307 (1984) 136.
42 B.M. Liu, H.C. Cheung and J. Mestecky, Biochemistry 20, (1981) 1997.
43 J. Slattery, D. Holowka and B. Baird, Biochemistry 24 (1985) 7810.
44 J. Holowka and R. Cathou, Biochemistry 15 (1976) 3379.
45 L.M. Chan and R.E. Cathou, J. Mol. Biol. 112 (1977) 653.
46 D.C. Hanson, R.C. Siegel and V.N. Schumaker, J. Biol. Chem. 260 (1985) 3576.
47 W.A. Wegener, Biopolymers 21 (1982) 1049.

48 D.C. Hanson, J. Yguerabide and V.N. Schumaker, Mol. Immun. 22 (1985) 237.
49 J. Reidler, V.T. Oi, W. Carlsen, T.M. Vuong, I. Pecht, I.A. Herenberg and L. Stryer, J. Mol. Biol. 158 (1982) 739.
50 E.I. Dudich, R.S. Nelyn and F. Frank, FEBS Lett. 89 (1978) 89.
51 R.A. Mendelson, M.F. Morales and J. Botts, Biochemistry 12 (1973) 2250.
52 S.C. Harvey and H.C. Cheung, Biochemistry 16 (1977) 5181.
53 T.P. Burghardt and N.L. Thompson, Biochemistry 24 (1985) 3731.
54 P. Wahl, K. Mihashi and J.C. Auchet, FEBS Lett. 60 (1975) 164.
55 K. Mihashi and P. Wahl, FEBS Lett. 52 (1975) 8.
56 S. Lowey, in: Subunits in biological systems, eds. S.N. Timasheff and G.D. Fasman (Dekker, New York, 1971) part A, ch. 5, p. 201.
57 M. Young, M.V. King, D. O'Hara and P.J. Molberg, Cold. Spring Harbor Symp. Quant. Biol. 37 (1972) 65.
58 M. Burke, S. Himmelfarb and W.F. Harrington, Biochemistry 12 (1973) 701.
59 M. Sassaroli, E. Bucci and R.F. Steiner, J. Biol. Chem. 257 (1982) 10136.
60 E. Bucci, C. Fronticelli, J. Flanigan, J. Perlman and R.F. Steiner, Biopolymers 18 (1979) 1261.
61 E. Antonini, E. Bucci, C. Fronticelli, E. Chiancone, J.C. Wyman and A. Rossi-Fanelli, J. Mol. Biol. 17 (1966) 29.
62 M. Sassaroli, J. Kowalczyck and E. Bucci, Arch. Biochem. Biophys. 251 (1986) 624.
63 J. Oton, D. Franchi, C. Fronticelli, R.F. Steiner, A. Martinez and E. Bucci, Arch. Biochem. Biophys. 228 (1984) 519.
64 J.R. Lakowicz, G. Laczko and I. Gryczynski, Rev. Sci. Instrum. 57 (1986) 2499.
65 E. Bucci, H. Malak, C. Fronticelli, I. Gryczynski and J.R. Lakowicz (1988) J. Biol. Chem., in the press.
66 J. Baldwin and C. Chothia, J. Mol. Biol. 129 (1979) 175.
67 J. Kowalczyk and E. Bucci, Biochemistry 22 (1983) 4805.
68 M. Sassaroli, E. Bucci, J. Liesegang, C. Fronticelli and R.F. Steiner, Biochemistry 23 (1984) 2487.
69 A.H. Chu and E. Bucci, J. Biol. Chem. 254 (1979) 371.
70 R. Cassoly, Methods Enzymol. 76 (1981) 121.
71 D. Franchi, C. Fronticelli and E. Bucci, Biochemistry 21 (1982) 6181.
72 M.F. Perutz, Annu. Rev. Biochem. 48 (1979) 327.
73 R.M. Hochstrasser and D.K. Negus, Proc. Natl. Acad. Sci. U.S.A. 81 (1984) 4399.